COBEM 2023 27TH INTERNATIONAL CONGRESS OF MECHANICAL ENGENEERING

ABCM Brazilian Society of Mechanical Sciences and Engineering
27th ABCM International Congress of Mechanical Engineering
December 04-08, 2023, Florianópolis-SC, Brazil

COB-2023-0203

A COMPARISON BETWEEN ANALYTICAL AND NUMERICAL RESULTS FOR THE PERFORMANCE OF A SMALL-SCALE SOLAR CHIMNEY

Cristiana Brasil Maia
Janaína de Oliveira Castro Silva
Matheus Augusto Ferreira Soares
Pontifícia Universidade Católica de Minas Gerais, Av. Dom José Gaspar, 500. Coração Eucarístico. 30535-901. Belo Horizonte, MG.
cristiana@pucminas.br; janainajocs@hotmail.com; maf.soares10@gmail.com

Elizaldo Domigues dos Santos
Universidade Federal do Rio Grande, Av. Itália, km 8, Carreiros, 96203-900 Rio Grande, RS

Abstract. *Solar chimneys are devices that use solar energy to generate a hot airflow. In large devices the airflow is used to run a wind turbine; nevertheless, great dimensions are required to generate power at competitive prices. Small prototypes are used to dry agricultural products or to provide natural ventilation. In this work, it was developed an unsteady analysis of the airflow inside a small-scale solar chimney. A mathematical model was developed for the temperature of the airflow at the outlet system, for the ground surface temperature, and for the mass flow rate reached by the airflow. It was also developed a CFD model for the airflow inside the system, based only on the ambient temperature, incident solar radiation, and wind speed. For both models, experimental data obtained from the Typical Meteorological Year (TMY) for Belo Horizonte, Brazil, were used. The results from analytical and numerical results were compared. It was observed that the ground surface temperature presented the lower differences between the models, and the outlet airflow temperature presented the higher differences. For the mass flow rate, the best results were found for the periods without solar radiation. This behavior can be attributed to simplifications of the analytical model.*

Keywords: *solar chimney, small-scale solar chimney, CFD, analytical model*

1. INTRODUCTION

The use and improvement of clean and renewable energy sources is an important topic to build less polluting civilizations and to supply the growing global electricity demand. It has been observed in the research on the use of renewable energy sources. Brazil is the 8th country in terms of scientific contributions on renewable energy studies, and the 1st in South America (Novas *et al*. 2021). Among the renewable energy sources, solar energy stands out as a clean and abundant source. Passive solar energy systems use heat or light directly from the sun, as in greenhouses. Active systems convert the energy from the sun into a more usable form, such as hot water or electricity.

Solar chimneys are devices that use solar energy to generate a hot airflow that can be used to run a wind turbine and generate electricity (Schlaich, 2002). Nevertheless, it has been proved that large-scale structures are required to generate power at competitive prices. Small-scale devices can be used for other purposes, such as for ventilation (Zhang *et al*. 2021) or to dry agricultural products (Maia *et al*. 2017).

Since the first pilot solar chimney power plant in 1982-83, several studies were performed, focusing on the development of mathematical models, numerical models, and experimental prototypes (Aliaga *et al*. 2021). Modified versions of solar chimneys have been proposed to enhance its energy utilization, such as combining energy production with desalination (Maia *et al*. 2019) and with energy production in PV panels (Tawalbeh *et al*. 2023).

Mathematical and numerical models are essentially different. Mathematical models are usually simpler and faster, providing more global results. Numerical models can solve the differential equations that govern the airflow, providing the fields of velocity and temperature inside the device. This work intends to compare the results of analytical and CFD models for the ground surface temperature, the outlet airflow temperature, and the mass flowrate of the airflow. The results were obtained on 8th February for a small-scale solar chimney located in Belo Horizonte, Brazil. The results were obtained based on experimental data of ambient temperature, wind speed, and solar radiation from the literature (Swera, n.d.). After the comparison, specific results for each model are also presented, such as the transient behavior expected for the airflow parameters for one year of simulation, using the analytical model, and detailed information on instantaneous velocity and temperature inside the solar chimney using the CFD model.

2. MATHEMATICAL MODEL

This paper presents a comparison between the results obtained in analytical and numerical models, for the ground surface and outlet airflow temperatures, and for the mass flow rate. This section presents the description of both models. The geometric parameters used in the mathematical model are presented in Figure 1. The dimensions hc and Rc represent, respectively, the collector height and radius. Ht and Dt represent, respectively, the tower height and diameter.

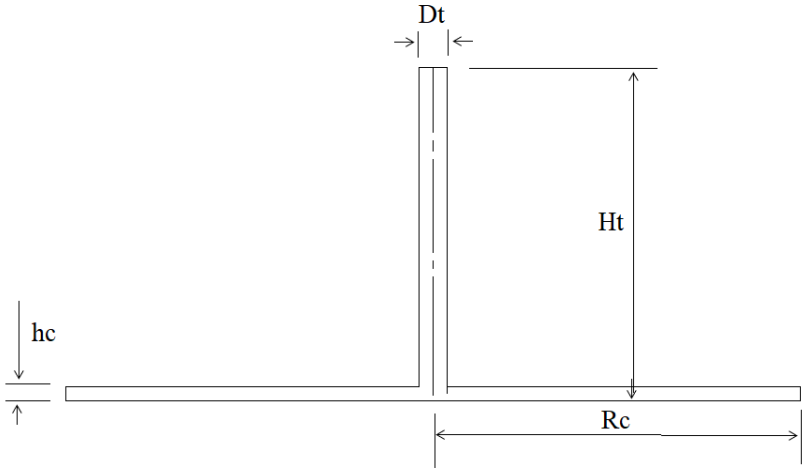

Figure 1. Schematic diagram of the solar chimney.

2.1 Analytical model

For large-scale solar chimneys, (Koonsrisuk *et al.* 2010) suggest an expression for the determination of the mass flow rate of the airflow, neglecting the difference between the collector and tower radius. However, for small-scale solar devices, this difference cannot be neglected. The mass flow rate is predicted by adapting the expression from (Koonsrisuk *et al.* 2010):

$$\dot{m} = \sqrt[3]{\frac{\frac{\rho^2 \beta' g q"_{conv,1} \pi^3}{8 C_p} H_t \left[{R_c}^2 - \left(\frac{D_t}{2}\right)^2 \right]}{\frac{4 F_y H_t}{{D_t}^5} + \frac{\frac{F_x}{64}}{R_c {h_c}^3} + \frac{1}{{D_t}^4}}} \tag{1}$$

ρ and C_p are the density and specific heat of the air, g is the gravity acceleration, β' is the volumetric expansion coefficient, F_x represents the friction factor in the collector, given by (Kröger and Burger, 2004)

$$F_x = 0.046\, {Re_x}^{-\frac{1}{5}} \tag{2}$$

F_y represents the friction factor in the tower.

$$\frac{1}{\sqrt{F_y}} = 1.5635\, ln\left(\frac{Re_x}{7}\right) \tag{3}$$

Re_x is the Reynolds number in the collector.
$q"_{conv,1}$ is the convective heat transfer between the ground and the airflow inside the collector, given by:

$$q"_{conv,1} = h_{ground,esc}\left(T_{ground} - T_{ao}\right) \tag{4}$$

The convective heat transfer coefficient between the ground surface and the flow $h_{ground,esc}$ is given by (Pretorius, 2007):

$$h_{ground,esc} = 3.87 + 0{,}0022\left(\frac{V \rho C_p}{Pr^{\frac{2}{3}}}\right) \tag{5}$$

Where T_{ao} is the average temperature of the air inside the collector, V is the average airflow velocity and Pr represents the Prandtl number of the air.

The average temperature of the airflow at the system outlet is given by (Ghalamchi *et al.* 2015).

$$T_{ao} = \frac{q"_{conv,1}\pi}{\dot{m}\, C_p}\left[{R_c}^2 - \left(\frac{D_t}{2}\right)^2\right] + T_{ai} \tag{6}$$

T_{ai} is the inlet air temperature, equal to the ambient temperature.

The ground surface temperature and the energy absorbed by the ground surface are determined by an energy balance developed by the heat transfer rates to the solar collector, represented schematically in Figure 2, described by (Maia and Castro Silva, 2022). The convective heat transfer rate between the solar collector and the airflow inside the system is $q"_{conv,3}$ and the radiative heat transfer rate between the solar collector and the ground is $q"_{rad,1}$. The collector loses heat to the environment by convection ($q"_{conv,2}$) and radiation ($q"_{rad,2}$).

The temperature in a specific depth of the ground can be determined by the solution of the one-dimensional unsteady energy conservation equation. Assuming the ground as a semi-infinite solid (Cristiana Brasil Maia 2005), the temperature of the ground surface is given by (Ozisik, 1993):

$$T_{ground}(t) = T_{ai} + \frac{2}{\sqrt{\pi}}\frac{\alpha'}{k_{ground}}\int_{t'=0}^{t} \frac{q"_{cond,0}(t')}{\sqrt{4\alpha'(t-t')}}dt' \tag{7}$$

α' is the thermal diffusivity of the ground. The conductive heat transfer to the ground is given by

$$q"_{cond,0} = -k_{ground}\frac{\partial T_{ground}}{\partial x}|_{x=0} \tag{8}$$

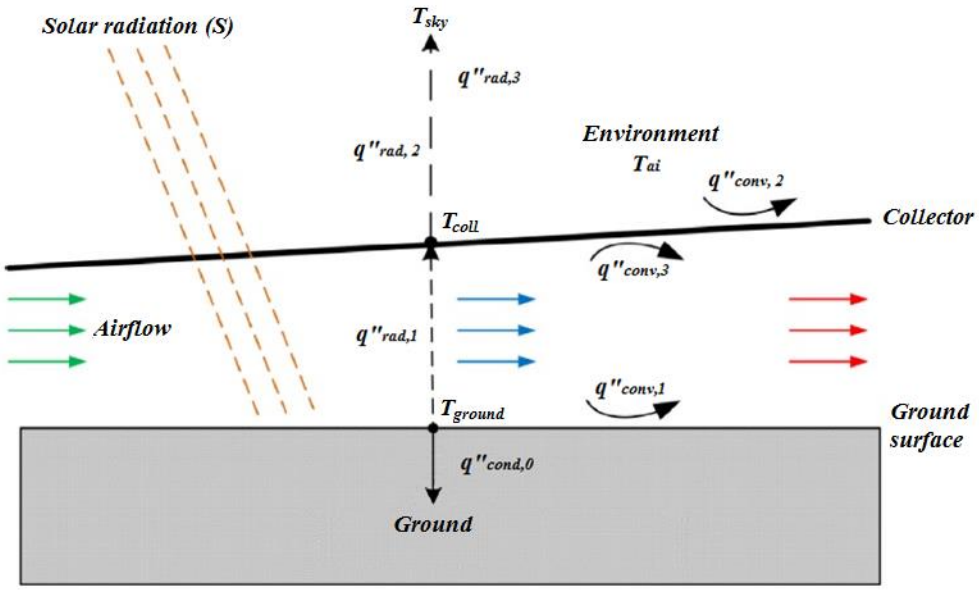

Figure 2. Energy balance.

The solar radiation absorbed by the ground is determined through an energy balance at the ground surface:

$$S - q"_{conv,1} - q"_{rad,1} - q"_{rad,3} = q"_{cond,0} \tag{9}$$

The radiative heat transfer between the ground surface and the solar collector$q"_{rad,1}$ can be assumed as the radiation between two infinite flat plates, as presented by (Duffie and Beckman, 2013).

$$q"_{rad,1} = \frac{\sigma\left({T_{ground}}^4 - {T_{coll}}^4\right)}{\frac{1}{\varepsilon_{coll}} + \frac{1}{\varepsilon_{ground}} - 1} \tag{10}$$

Where ε_{coll} and ε_{ground} represent the collector and ground emittance, respectively. T_{coll} represent the surface collector temperature.

The radiative heat transfer rate between the ground and the environment can be estimated by

$$q"_{rad,3} = \tau_{coll}\,\sigma\varepsilon_{ground}\left({T_{ground}}^4 - {T_{sky}}^4\right) \tag{11}$$

τ_{coll} is the infrared transmittance of the collector.

Considering an isotropic sky model, the absorbed energy by the ground is the sum of the beam (I_b), diffuse (I_d) and ground-reflected components, as given by (Duffie and Beckman, 2013)

$$S = I_b R_b(\tau\alpha)_b + I_d R_d\left(\frac{1+cos\,\beta}{2}\right) + \rho_g I(\tau\alpha)_g\left(\frac{1-cos\,\beta}{2}\right) \tag{12}$$

$(\tau\alpha)$ represents the transmittance-absorptance for the beam (subscript b), diffuse (subscript d) and ground reflected (subscript g) components. β is the tilt angle of the collector (in this work, $\beta = 0°$). ρ_g is the ground reflectance, and R_b represents the ratio between the solar radiation on a tilted surface and on a horizontal surface.

A complete description of the model is presented in (Maia and Castro Silva, 2022). Radiative heat transfers were modeled following classic models from literature, as suggested by (Duffie and Beckman, 2013). Convective heat transfer coefficients were adopted according to the literature on solar chimneys (Pretorius, 2007; Li *et al.* 2012).

2.2 Numerical model

In this section, the differential equations for the conservation of mass, momentum, and energy (Versteeg and Malalasekera, 2007; Bejan, 2013) are presented.

$$\frac{\partial\rho}{\partial t} + \nabla\,(\rho\cdot\vec{v}) = 0 \tag{13}$$

$$\frac{\partial}{\partial t}(\rho\cdot\vec{v}) + \nabla\,(\rho\cdot\vec{v}\cdot\,\vec{v}) = -\nabla p + \nabla\,\left(\mu\left[(\nabla\vec{v} + \nabla\vec{v}^T) - \frac{2}{3}\nabla\cdot\vec{v}\,I\right]\right) + \rho\,\vec{g} \tag{14}$$

$$\frac{\partial}{\partial t}(\rho E) + \nabla\,\cdot\left(\vec{v}(\rho E + p)\right) = \nabla\left(k_{eff}\nabla T - h\vec{J} + \left(\mu\left[(\nabla\vec{v} + \nabla\vec{v}^T) - \frac{2}{3}\nabla\cdot\vec{v}\,I\right]\cdot\vec{v}\right)\right) \tag{15}$$

In previous equations, t stands for time, ρ for density, $\vec{v}$ for velocity, p for pressure, E for energy, and $\vec{g}$ for gravity.

The airflow inside the solar chimney is turbulent, therefore, it is necessary to take into account turbulent effects. To tackle with closure model, the k-ε turbulence model was used, being the turbulent viscosity given by:

$$\mu_t = \rho C_\mu \frac{k^2}{\varepsilon} \tag{16}$$

C_μ, k and ε represent an empirical constant, the turbulent kinetic energy, and the rate of dissipation of the turbulent kinetic energy, respectively. The main equations for the turbulence model are given by (Launder and Spalding, 1974).

The k-ε turbulence model is the most used model for the study of solar chimneys (Maia *et al*. 2009; Yazdi *et al*. 2021; Gholamalizadeh and Kim, 2016). Also, in an evaluation of the effect of the turbulence model on the simulation of solar chimneys, this model showed the best agreement with experimental results among the evaluated models (Ayadi *et al*. 2018).

The airflow inside the solar chimney is induced by natural convection. The Rayleigh number is the dimensionless parameter that measures the intensity of the flow. It is defined by:

$$Ra = \frac{g\beta\Delta T h_c^3}{\alpha\nu} \tag{17}$$

ΔT is the maximum temperature increase within the system. α is the thermal diffusivity, ν is the kinematic viscosity, β is the thermal expansion coefficient.

3. MATERIALS AND METHODS

Figure 1 shows the physical model used for the small-scale solar chimney. The Manzanares pilot plant served as a reference (1:50 scale) for the model, defined as the same dimensions of an experimental prototype built in Belo Horizonte, Brazil (Maia and Castro Silva, 2022). The tower height and diameter are, respectively, 2.50 m and 0.20 m, and the collector height and diameter are, respectively, 0.10 m and 5.0 m.

Experimental data from the Typical Meteorological Year (TMY) obtained from the literature (Swera, n.d.) were used as input data for the simulation. The numerical results were obtained for one day, considering a timestep of 1 hour. Ambient temperature, wind speed, and solar radiation were collected for February 8th. With these values, the heat absorbed by the ground was determined using Eq. 9. Table 1 presents the input data.

Table 1. Data of heat flux, ambient temperature, and wind speed on February 8th in Belo Horizonte, Brazil.

Time (h)	Heat flux (W/m^2)	Ambient temperature (K)	Wind speed (m/s)
1:00	0	295.7	0
2:00	0	295.3	0
3:00	0	295.1	0
4:00	0	294.1	0
5:00	25.8	294.1	0
6:00	121.4	299.1	0
7:00	251.7	300.1	0
8:00	381.4	300.6	3.6
9:00	489.7	301.5	4.1
10:00	565.0	302.3	5.1
11:00	591.7	303.0	2.6
12:00	565.0	303.5	3.6
13:00	489.7	303.8	4.1
14:00	381.4	304.0	5.1
15:00	251.7	304.1	5.1
16:00	121.4	304.0	5.1
17:00	25.8	303.6	5.1
18:00	0	303.0	3.8
19:00	0	302.4	2.6
20:00	0	301.8	1.5
21:00	0	301.3	0.7
22:00	0	300.7	0
23:00	0	300.2	0
24:00	0	297.2	0

In this study, ANSYS CFX® 14.5 software (ANSYS, 2013)was used for simulation. The computational domain used includes three different domains: the solar chimney, the ground, and the atmosphere, as indicated in Figure 3.

The mesh was defined after a mesh test, in which three mesh configurations were evaluated. The most refined one, with 117,137 nodes and 525,792 elements, was used for obtaining the results. The mesh consists of tetrahedral elements inside the geometry and prism elements on the walls, as suggested by (Menter *et al*. 2002).

The atmosphere around the solar chimney was modeled as a parallelepiped 10 m in width and 5 m in height, with air as a real gas, atmospheric pressure of 91.5 kPa (for the city of Belo Horizonte, Brazil), and ambient temperature given in Table 1. The upper and lower surface of the atmosphere were considered adiabatic. In the lateral surfaces, an opening condition was assumed, allowing the air to enter or leave the system. In one of the lateral faces, it was assumed a prescribed value for the wind speed, obtained experimentally (Table 1). The boundary conditions are schematically presented in Figures 3 and 4.

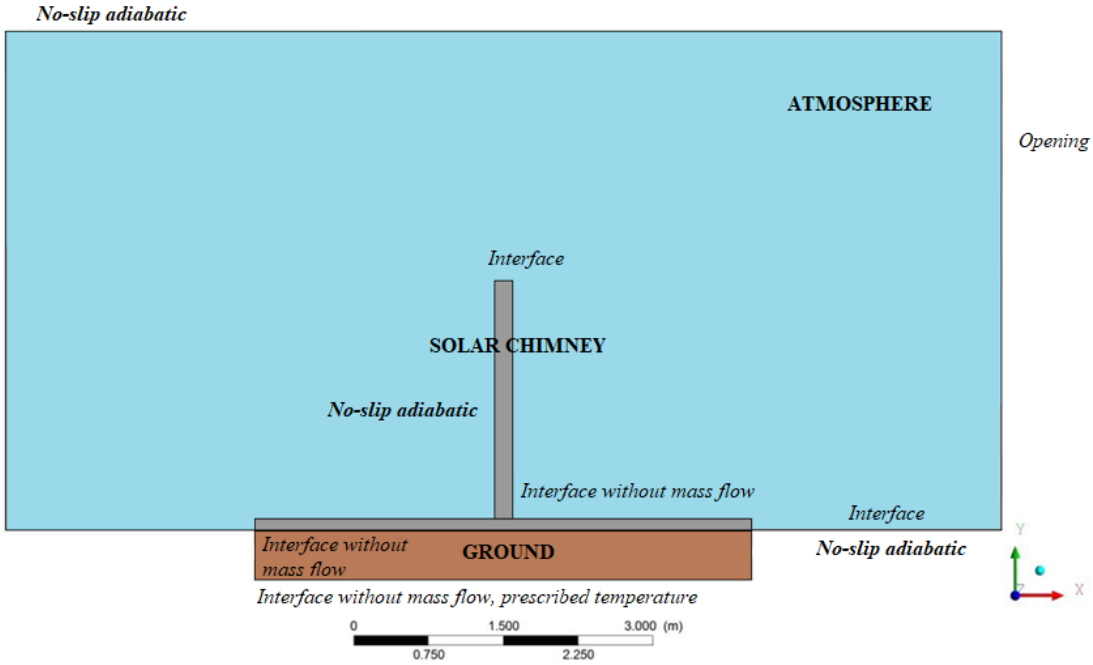

Figure 3. Computational domain.

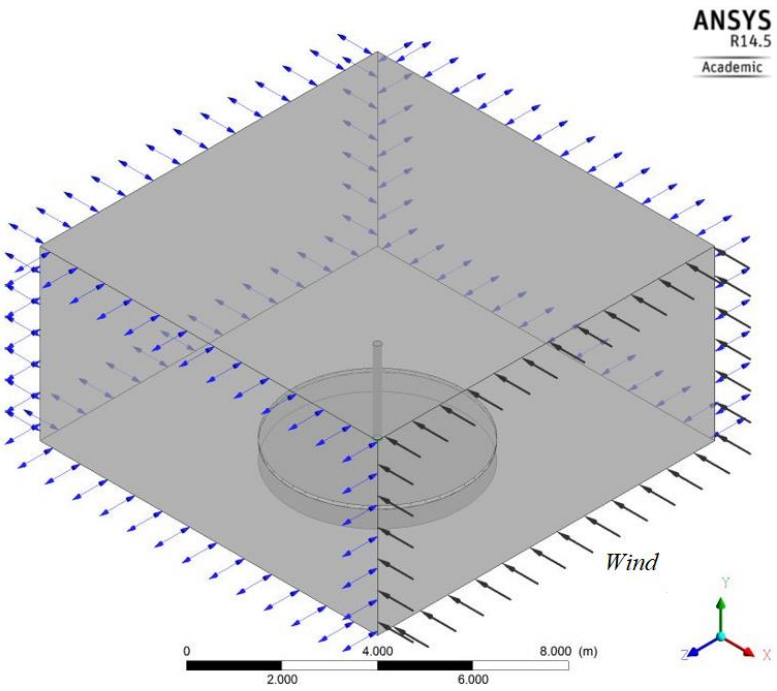

Figure 4. Boundary conditions.

Since the airflow is generated by buoyancy forces, the velocity in the radial direction is unknown (Maia *et al*. 2009), depending on the ambient conditions. The use of a computational box representing the atmosphere, as presented by (RahimiLarki *et al*. 2021) avoids the prescription of the velocity at the collector inlet. The velocity is obtained by the solution of the governing equations.

The ground was modeled as a continuous solid of brick, with 0.5 m of depth. At the beginning of the simulation, it was assumed a homogeneous temperature, equal to the ambient temperature. On the bottom surface, a no-slip condition and a fixed value for the temperature were considered. In the lateral surface, it was assumed a no-slip adiabatic condition.

The tower wall was assumed adiabatic. The inlet and outlet of the solar chimney were modeled as opening conditions. The collector surface and the ground surface were modeled as an interface without mass flow, allowing only energy

transfers. At the ground surface, a prescribed value for the heat flux was adopted, corresponding to the absorbed energy from the ground, determined by Eq. (9).

4. RESULTS

The results are presented for 8th February. The energy absorbed by the ground surface is the difference between the incident solar radiation on the collector surface and thermal and optical losses, as previously described. Figure 5 presents the incident solar radiation and the portion absorbed by the ground surface throughout the day. As expected, as it was a clear day, the energy absorbed followed the incident solar radiation behavior, but with smaller values.

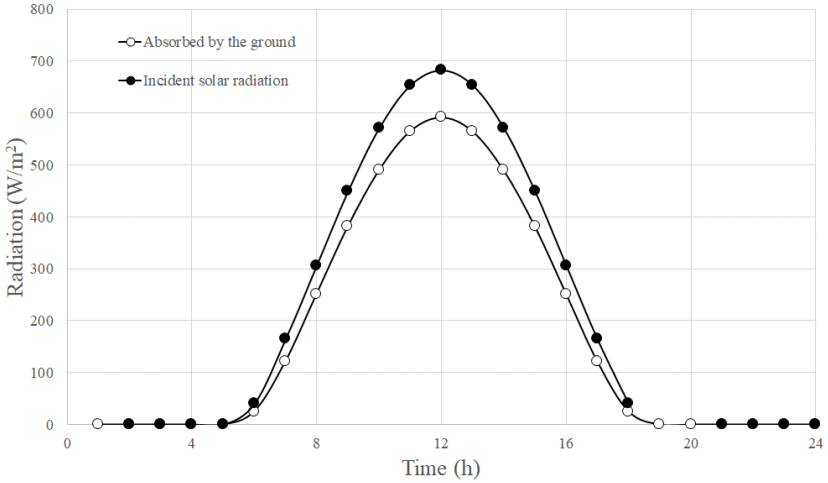

Figure 5. Incident and absorbed energy flux.

The energy absorbed by the ground surface and experimental data from 8th February were used to run the analytical and CFD models, resulting in hourly values for the ground surface temperature (Fig 6), outlet airflow temperature (Fig 7), and mass flow rate (Fig 8).

The analytical and numerical values for the ground surface temperature did not show significant variations. However, great differences were obtained for the outlet airflow temperatures. The discrepancies may be explained by the equations solved by both models. The analytical model uses theoretical equations from the literature for the outlet temperature, while the CFD model solves the conservation equations based on the other variables. For the ground surface temperature, the analytical model uses an energy balance, resulting in lower differences. Experimental results are not presented since no measurements were performed for this particular day. For other days, experimental results obtained in this prototype can be seen in (Maia & Castro Silva, 2021)

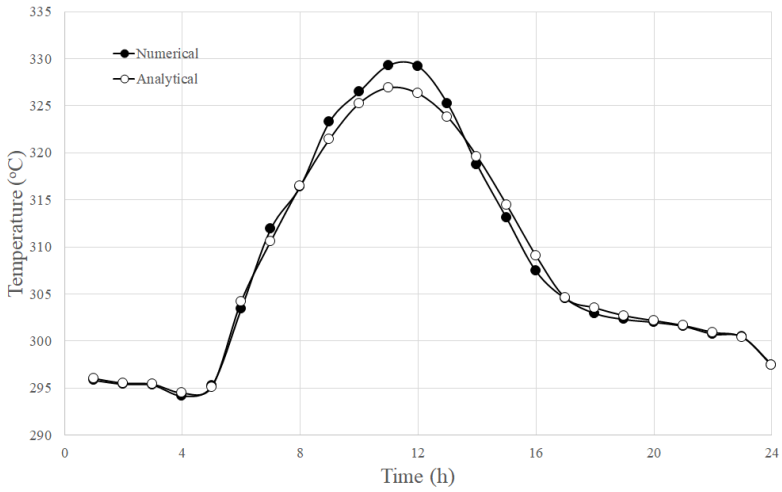

Figure 6. Comparison between analytical and numerical results of ground surface temperature.

The predictions for the mass flow rate were similar during the period of solar incidence, but at night, the CFD model resulted in higher values. The differences may again be attributed to the equations solved by each model. It is expected the CFD predictions to be more accurate.

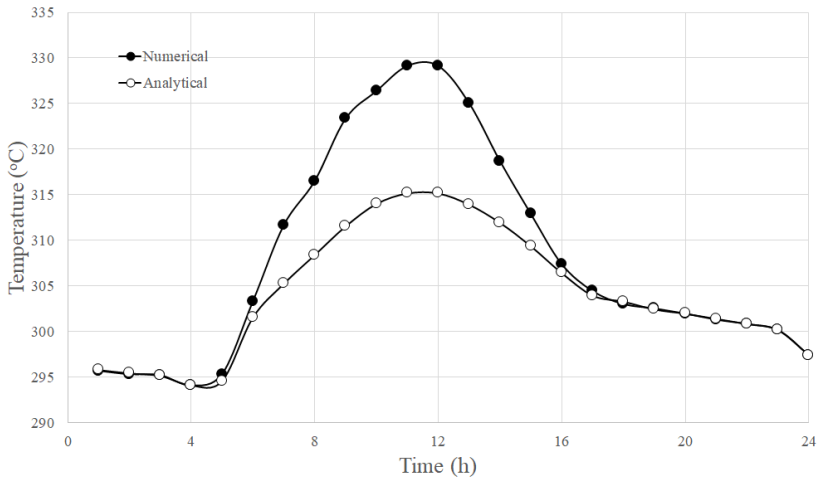

Figure 7. Comparison between analytical and numerical results of outlet airflow temperature.

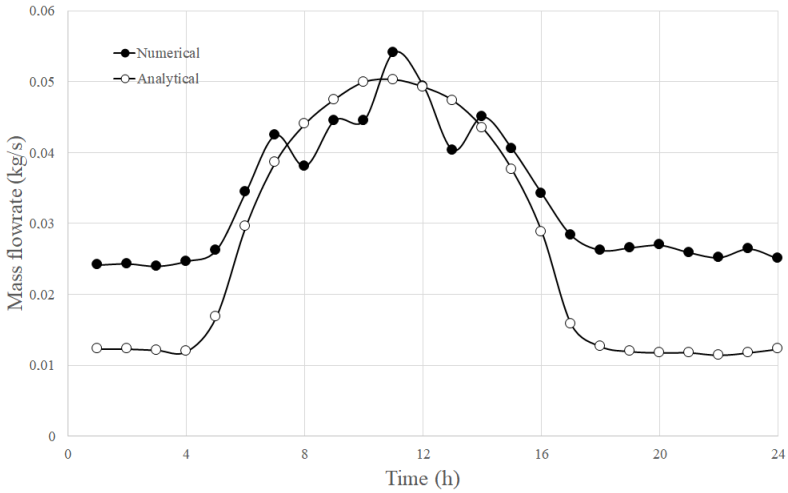

Figure 8. Comparison between analytical and numerical results of mass flow rate.

It is interesting to evaluate some specific results from both models. The analytical model was able to predict the airflow parameters for the entire year, allowing the assessment of the annual behavior of the solar chimney. Figure 9a presents the monthly averaged values of the outlet airflow and ground surface temperatures, and Figure 9b presents the monthly averaged mass flow rate and heat absorbed by the airflow. The CFD model was able to predict the temperature and velocity fields inside the computational domain.

The airflow inside a solar chimney is generated by buoyancy forces created when the air inside the solar collector is heated by the ground surface, heated by the incident solar energy. It is expected, therefore, the ground surface temperature to be higher than the outlet airflow temperature, and the airflow temperature to be higher than the ambient temperature since the air enters the solar chimney at ambient temperature. This behavior is observed in Figure 9, which shows the monthly averaged values for these temperatures. On average, the temperature of the ground surface temperature was 4°C higher than the outlet airflow, which was 4°C higher than the ambient. It is worth noting that during the day, the differences were more significant.

The heat absorbed by the ground is a direct consequence of the incident solar radiation over the solar collector. In the southern hemisphere, the solar incidence is higher from September to March, corresponding to spring and summer. As can be seen in Figure 9, the heat absorbed by the ground is higher in this period. The driving force for the airflow generation is the ground surface temperature, which presents a similar behavior to the heat absorbed by the ground. The behavior of the mass flow rate is also similar. The smaller variations may be attributed to the increase of the viscous

forces for higher ground temperatures. Again, it is worth noting that the daily variations of the mass flow rate were more significant.

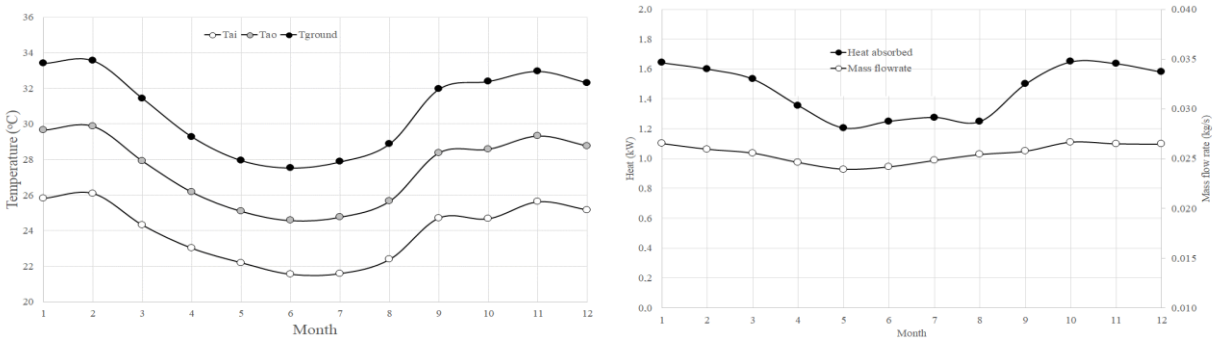

(a) (b)

Figure 9. Temperatures (a), heat absorbed (b), and mass flow rate (b) predicted for one year of simulation.

5. CONCLUSIONS

In this present work, it was assessed the airflow inside a small-scale solar chimney. Experimental results from the TMY for Belo Horizonte, Brazil, were used as input data to run analytical and numerical models for ground surface temperature, outlet airflow temperature, and mass flow rate of a solar chimney operating in this city. In the analytical model, consolidated correlations from literature were used, combined with an energy balance. In the numerical model, a CFD analysis was developed, using as boundary conditions the ambient temperature, the incident solar radiation, and the wind speed.

In general, the ground surface temperature and the mass flow rate were similar for both models, but the outlet airflow temperature presented higher differences for the models. The differences may be attributed to the set of equations solved. While the analytical model used general equations, in the numerical model the governing equations were solved, leading to more accurate results.

Using estimated values for the incident solar radiation, wind speed and ambient temperature, it was possible to simulate the behavior of a small-scale solar chimney for one year. As expected, the heat absorbed by the airflow, the mass flowrate and the airflow temperatures were higher from September to March, and lower from April to August. When compared the ground surface and outlet airflow temperatures, ground surface temperature was 4℃ higher than the outlet airflow, which was 4℃ higher than the ambient. It is worth noting that during the day, the differences were more significant.

6. ACKNOWLEDGEMENTS

This study was financing in part by the Coordenação de Aperfeiçoamento de Pessoal de Nível Superior - Brasil (CAPES) - Finance Code 001. The authors are also thankful to PUC Minas, FURG, FAPEMIG (PPM 00650-18), and CNPq 444864/2020-2, 308396/2021-9 and 302175/2022-9.

7. REFERENCES

Aliaga, D. M., R. Feick, W. K. Brooks, M. Mery, R. Gers, J. F. Levi, and C. P. Romero. 2021. “Modified Solar Chimney Configuration with a Heat Exchanger: Experiment and CFD Simulation.” *Thermal Science and Engineering Progress* 22. https://doi.org/10.1016/j.tsep.2021.100850.

Ayadi, Ahmed, Haithem Nasraoui, Abdallah Bouabidi, Zied Driss, Moubarak Bsisa, and Mohamed Salah Abid. 2018. “Effect of the Turbulence Model on the Simulation of the Air Flow in a Solar Chimney.” *International Journal of Thermal Sciences* 130. https://doi.org/10.1016/j.ijthermalsci.2018.04.038.

ANSYS. (2013). *CFX. Solver Theory Manual 14.5*.

Bejan, Adrian. 2013. *Convection Heat Transfer: Fourth Edition*. *Convection Heat Transfer: Fourth Edition*. https://doi.org/10.1002/9781118671627.

Duffie, John A., and William A. Beckman. 2013. *Solar Engineering of Thermal Processes: Fourth Edition*. *Solar Engineering of Thermal Processes: Fourth Edition*. https://doi.org/10.1002/9781118671603.

Ghalamchi, Mehran, Alibakhsh Kasaeian, and Mehrdad Ghalamchi. 2015. “Experimental Study of Geometrical and Climate Effects on the Performance of a Small Solar Chimney.” *Renewable and Sustainable Energy Reviews*. https://doi.org/10.1016/j.rser.2014.11.068.

Gholamalizadeh, Ehsan, and Man Hoe Kim. 2016. "CFD (Computational Fluid Dynamics) Analysis of a Solar-Chimney Power Plant with Inclined Collector Roof." *Energy* 107. https://doi.org/10.1016/j.energy.2016.04.077.

Koonsrisuk, A., S. Lorente, and A. Bejan. 2010. "Constructal Solar Chimney Configuration." *International Journal of Heat and Mass Transfer* 53 (1–3): 327–33. https://doi.org/10.1016/j.ijheatmasstransfer.2009.09.026.

Kröger, D.G., and M. Burger. 2004. "Experimental Convection Heat Transfer Coefficient on a Horizontal Surface Exposed to the Natural Environment." In *Proceedings of the ISES EuroSun2004 International Sonnenforum*, 422–30.

Launder, B. E., and D. B. Spalding. 1974. "The Numerical Computation of Turbulent Flows." *Computer Methods in Applied Mechanics and Engineering* 3 (2). https://doi.org/10.1016/0045-7825(74)90029-2.

Li, Jing yin, Peng hua Guo, and Yuan Wang. 2012. "Effects of Collector Radius and Chimney Height on Power Output of a Solar Chimney Power Plant with Turbines." *Renewable Energy* 47: 21–28. https://doi.org/10.1016/j.renene.2012.03.018.

Maia, Cristiana B., André G. Ferreira, Ramón M. Valle, and M. F B Cortez. 2009. "Theoretical Evaluation of the Influence of Geometric Parameters and Materials on the Behavior of the Airflow in a Solar Chimney." *Computers and Fluids* 38 (3): 625–36. https://doi.org/10.1016/j.compfluid.2008.06.005.

Maia, Cristiana B., Felipe V.M. Silva, Vinícius L.C. Oliveira, and Lawrence L. Kazmerski. 2019. "An Overview of the Use of Solar Chimneys for Desalination." *Solar Energy* 183 (May): 83–95. https://doi.org/10.1016/j.solener.2019.03.007.

Maia, Cristiana Brasil. 2005. "Análise Teórica e Experimental de Uma Chaminé Solar: Avaliação Termofluidodinâmica." Universidade Federal de Minas Gerais.

Maia, C. B., & Castro Silva, J. de O. (2021). Experimental Analysis of a Modular Solar Chimney. 26th International Congress of Mechanical Engineering. https://doi.org/10.26678/abcm.cobem2021.cob2021-0372

Maia, Cristiana Brasil, and Janaína de Oliveira Castro Silva. 2022. "Thermodynamic Assessment of a Small-Scale Solar Chimney." *Renewable Energy* 186: 35–50. https://doi.org/10.1016/j.renene.2021.12.128.

Maia, Cristiana Brasil, André Guimarães Ferreira, Luben Cabezas-Gómez, Janaína de Oliveira Castro Silva, and Sérgio de Morais Hanriot. 2017. "Thermodynamic Analysis of the Drying Process of Bananas in a Small- Scale Solar Updraft Tower in Brazil." *Renewable Energy* 114: 1005–12. https://doi.org/10.1016/j.renene.2017.07.102.

Menter, F.R., B. Hemstrom, M. Henriksson, R. Karlsson, A. Latrobe, A. Martin, P. Muhlbauer, et al. 2002. "CFD Best Practice Guidelines for CFD Code Validation for Reactor-Safety Applications." *Evol– Ecora – D 01*.

Novas, Nuria, Rosa María Garcia, Jose Manuel Camacho, and Alfredo Alcayde. 2021. "Advances in Solar Energy towards Efficient and Sustainable Energy." *Sustainability (Switzerland)* 13 (11). https://doi.org/10.3390/su13116295.

Ozisik, M N. 1993. "Heat Conduction." *Book*.

Pretorius, Johannes Petrus. 2007. "Optimization and Control of a Large-Scale Solar Chimney Power Plant." University of Stellenbosch.

RahimiLarki, Mohsen, Reza Hosseini Abardeh, Hassan Rahimzadeh, and Hamid Sarlak. 2021. "Performance Analysis of a Laboratory-Scale Tilted Solar Chimney System Exposed to Ambient Crosswind." *Renewable Energy* 164. https://doi.org/10.1016/j.renene.2020.10.118.

Schlaich, J. 2002. "The Solar Chimney: Electricity from the Sun." Stuttgart.

Maia, C. B., & Castro Silva, J. de O. (2021). Experimental Analysis of a Modular Solar Chimney. *26th International Congress of Mechanical Engineering*. https://doi.org/10.26678/abcm.cobem2021.cob2021-0372

Swera. (n.d.). *Solar and Wind Energy Resource Assessment (SWERA)*. Retrieved November 8, 2018, from https://openei.org/apps/SWERA//

Tawalbeh, Muhammad, Shima Mohammed, Aaesha Alnaqbi, Shouq Alshehhi, and Amani Al-Othman. 2023. "Analysis for Hybrid Photovoltaic/Solar Chimney Seawater Desalination Plant: A CFD Simulation in Sharjah, United Arab Emirates." *Renewable Energy* 202. https://doi.org/10.1016/j.renene.2022.11.106.

Versteeg, H K, and W Malalasekera. 2007. *An Introduction to Computational Fluid Dynamics: The Finite Volume Method*. Pearson Education Limited.

Yazdi, M. H., E. Solomin, A. Fudholi, K. Sopian, and P. L. Chong. 2021. "Numerical Analysis of the Performance of a Hybrid Solar Chimney System with an Integrated External Thermal Source." *Thermal Science and Engineering Progress* 26. https://doi.org/10.1016/j.tsep.2021.101127.

Zhang, Haihua, Dong Yang, Vivian W.Y. Tam, Yao Tao, Guomin Zhang, Sujeeva Setunge, and Long Shi. 2021. "A Critical Review of Combined Natural Ventilation Techniques in Sustainable Buildings." *Renewable and Sustainable Energy Reviews*. Elsevier Ltd. https://doi.org/10.1016/j.rser.2021.110795.

8. RESPONSIBILITY NOTICE

The authors are the only responsible for the printed material included in this paper.